Karlsruhe Institute of Technology

Institute for Applied Materials

UNSW AUSTRALIA

School of Materials Science & Engineering

# Strain mechanisms in actuators: in operando investigation of functional materials

M. Hinterstein[1,2], M. Hoelzel[3], J. Rouquette[4], A. Studer[5] and M. Hoffman[2]

[1]Institute for Applied Materials, Karlsruhe Institute for Technology, P.O. Box 3640, 76021 Karlsruhe, Germany

[2]School of Materials Science and Engineering, UNSW Australia, 2052 Sydney, Australia

[3]Forschungsneutronenquelle Heinz-Maier-Leibnitz (FRM II), Technische Universität Muenchen, Lichtenbergstr. 1, 85747 Garching, Germany

[4]Institut Charles Gerhardt UMR CNRS 5253 Equipe C2M, Universit Montpellier II, Place Eugene Bataillon, cc1504, 34095 Montpellier cedex 5, France

[5]Bragg Institute, Australian Nuclear Science and Technology Organisation, Locked Bag 2001, Kirrawee, NSW2234, Australia

## Motivation

Functional materials which perform a designed action in response to an environmental stimulus are becoming increasingly valuable in the design of novel devices and technologies. An important class of functional materials are piezoelectric perovskites. Their extraordinary (and well-known) ability to couple elastic strain and polarization under the influence of an applied electric field is exploited in piezoelectric sensors, actuators and for energy harvesting. Prominent examples are multilayer stack actuators used in a large number of every-day and high-tech applications, e.g.:

- In ink-jet printers to increase efficiency[1].
- In modern combustion engines for automobiles to control fuel injection cycles[2].
- In trains, planes or cars they are used for active vibration damping to guarantee comfortable travelling[3].
- In modern highly dynamic gantry type machine tools, piezoelectric actuators are used for active error compensation of structural oscillations at the tool centre point[4].

In the past decade *in situ* and *in operando* techniques for the investigation of piezoceramics advanced signicantly[5,6]. However, to date the literature does not provide a method to correlate all structural mechanisms with the macroscopic observations. Here we present a comprehensive model, which is capable of describing the macroscopic behaviour based on a model on the atomic scale[7].

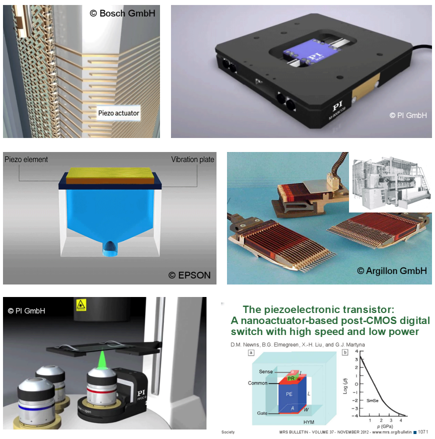


## Experimental (measurement)

Special requirements are necessary for a successful X-ray or neutron diffraction analysis. In order to resolve the coexisting and highly correlated phases, a high angular resolution is mandatory. At the same time a high Q-range is necessary to obtain enough information to correctly determine the orientation distribution function (ODF) of the textured material. The requirements could be achieved with neutron diffraction measurements at high-intensity neutron diffractometers such as D20[8] (Institute Laue-Langevin, Grenoble) or WOMBAT[9] (Australian Nuclear Science and Technology Organisation). For each measurement, a series of 13 complete diffraction patterns were collected with different orientations of the electric field with respect to the incident beam by moving the ω-sample table in 15° steps. By this means, the relative orientation between the electric field vector and the scattering vectors of the individual reflections was varied.

- No limitation due to absorption
- Full orientation series possible ($0° \leq \omega \leq 180°$)
- Fast measurement at beamlines like D20 (ILL) or WOMBAT (ANSTO)

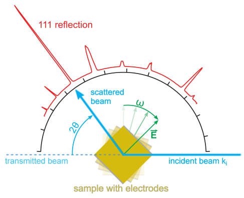


## Experimental (analysis)

Data analysis was carried out using the software package MAUD (Materials Analysis Using Diffraction)[10]. MAUD allows full pattern Rietveld refinements including full texture analysis for multiple phases. Therefore, all data sets with different sample orientations contribute to the refinement. By assigning the Euler angles of the experiment to each diffraction pattern, the orientation dependent information can be exploited. For this additional information the extended Williams-Imhof-Matthies-Vinel (E-WIMV) algorithm was used for texture refinement[11] and the weighted strain orientation distribution function (WSODF) strain model for refinement of the field induced lattice strain[12]. The phase fractions can be obtained from Rietveld refinement.

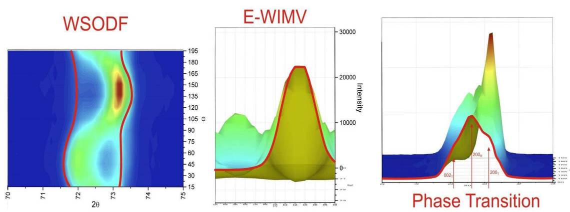


- Weighted Strain Orientation Distribution Function → lattice strain / piezoelectric effect
- E-WIMV: discrete method to obtain ODF → domain switching
- Refinement of scale factors → phase fractions

## PIC 151 ($Pb_{0.99}[Zr_{0.45}Ti_{0.47}(Ni_{0.33}Sb_{0.67})_{0.08}]O_3$)

## BNT-25ST ($0.75Bi_{½}Na_{½}TiO_3 – 0.25SrTiO_3$)

The *in situ* neutron diffraction patterns of a commercial ferroelectric material PIC151 and a incipient relaxor ferroelectric material BNT-25ST show all three field induced strain mechanisms, namely domain switching, lattice strain and phase transition. In the MAUD software all instrumental and sample orientation angles can be assigned to the individual patterns. The final refinement consists of a regular Rietveld refinement based on a structure model and additional model parameters for strain and texture for each phase. The figures below depict the measured and calculated patterns with insets of the $111_C$ and $200_C$ reflections for the remanent and the applied field state. The comparison of the measured data and the patterns calculated from the fitted parameters shows the accurate modelling of the diffraction patterns.

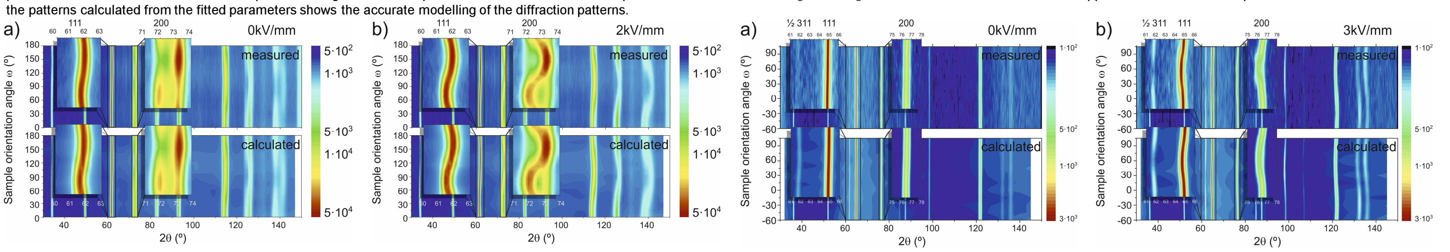


## Comparison of model and measurement

Macroscopic measurement: 10mHz

Diffraction model: 16μHz

→ Dynamic contribution?

Creep in PIC 151:

600s at 2kV/mm: 0.05%[13]

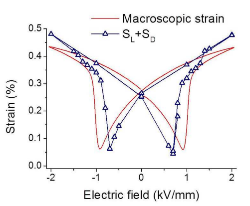


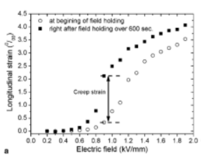


## Strain calculation

From the orientation distribution function, the lattice strain model and the phase fractions, the macroscopic strain response can be calculated. This way a quantification of the strain mechanisms is possible.

While PIC151 exhibits a significant remanent lattice and domain strain, BNT-25ST shows almost no remanent strain at all. However, the field induced strain in BNT-25ST is significantly higher than the field induced strain of PIC151.

The evaluation of the strain behaviour of both systems reveals fundamental differences. While PIC151 is dominated by the lattice strain of the rhombohedral phase, BNT-25ST is dominated by the lattice strain of the tetragonal phase. In BNT-25ST both phases show a pronounced domain strain, while PIC151 only exhibits tetragonal domain strain.

### PIC151

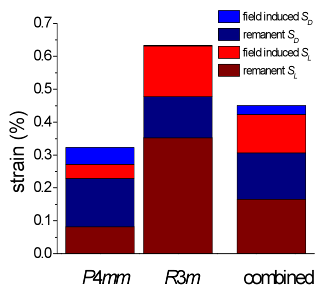


### BNT-25ST

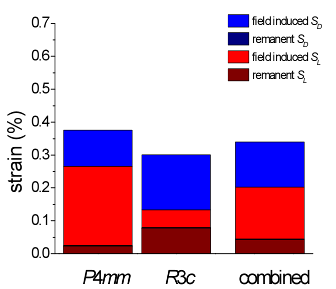


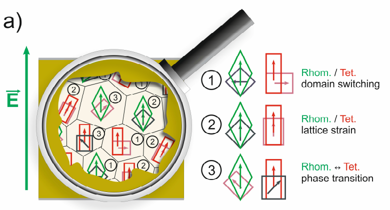


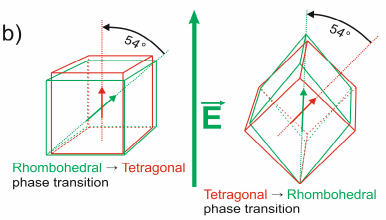


## Strain mechanisms

These new insights in the strain mechanisms of actuator materials explain the strong effect of phase boundaries on the piezoelectric properties. In the vicinity of a phase boundary, the activation energy of a phase transition is low enough so that the applied electric field can induce the transition in both directions, depending on grain orientation. Thus, the material can benefit from all polarization directions of the involved phases. These additional directions result in a formerly unknown 54° domain switching between tetragonal and rhombohedral symmetry and explain the exceptional strain behaviour of morphotropic compositions.

## Funding

- Feodor Lynen program of the Alexander von Humboldt Foundation
- BMBF project 05K13VK1
- Discovery Early Career Research Award of the Australian Research Council (DE150100750)

## References

1. Wu, H.-C., Shan, T.-R., Hwang, W.-S. & Lin, H.-J., *Mater. Trans.* **45**, 1794–1801 (2004).
2. Randall, C. A., Kelnberger, A., Yang, G. Y., Eitel, R. E. & Shrout, T. R., *J. Electroceramics* **14,** 177–191 (2005).
3. Lee, J., Kim, J. & Cheong, C. C., *J. Mater. Sci. Technol.* **13,** 451–458 (1999).
4. Stöppler, G. & Douglas, S., *Mechatronics* **18,** 426–433 (2008).
5. Hinterstein, M., Rouquette, J., Haines, J., Papet, P., Knapp, M., Glaum, J. & Fuess, H., *Phys. Rev. Lett.* **107,** 077602 (2011).
6. Hinterstein, M., Rouquette, J., Haines, J., Papet, P., Glaum, J., Knapp, M., Eckert, J. & Hoffman, M., *Phys. Rev. B* **90,** 094113 (2014).
7. Hinterstein, M., Hoelzel, M., Rouquette, J., Haines, J., Glaum, J., Kungl, H. & Hoffman, M., *Acta Mater.* **94**, 319-327 (2015).
8. Hansen, T. C., Henry, P. F., Fischer, H. E., Torregrossa, J. & Convert, P., *Meas. Sci. Technol.* **19,** 034001 (2008).
9. Studer, A. J., Hagen, M. E. & Noakes, T. J., *Phys. B Condens. Matter* **385-386,** 1013–1015 (2006).
10. Matthies, S., Lutterotti, L. & Wenk, H. R., *J. Appl. Crystallogr.* **30,** 31–42 (1997).
11. Matthies, S., Wenk, H.-R. & Vinel, G. W., *J. Appl. Crystallogr.* **21,** 285–304 (1988).
12. Popa, N. C. & Balzar, D., *J. Appl. Crystallogr.* **34,** 187–195 (2001).
13. Zhou, D. & Kamlah, M., *Acta Mat.* **54**, 1389 (2006).